

Litter nutrient contents controls extend of lignin decomposition via decomposer community composition in Beech litter

Lukas Kohl¹, Wolfgang Wanek¹, Katharina Keiblinger^{2,3}, Sonja Leitner^{1,3}, Maria Mooshammer¹, Ieda Hämmerle¹, Lucia Fuchslueger¹, Jörg Schneckner¹, Thomas Schneider^{4,5}, Sandra Moll⁷, Markus Gorfer^{7,8}, Joseph Strauss^{7,8}, Katharina Riedel^{4,6}, Leo Eberl^{4,5}, Sophie Zechmeister-Boltenstern^{2,3}, Andreas Richter¹,

1 Department of Chemical Ecology and Ecosystem Research, University of Vienna, Althanstrasse 14, A-1090 Vienna, Austria

2 Federal Research and Training Centre for Forests, Natural Hazards and Landscape, Department of Soil Biology, Seckendorff-Gudent-Weg 8, A-1131 Vienna, Austria

3 Current address: Institute for Soil Science, University of Natural Resources and Life Sciences, Peter Jordan-Straße 82, A-1180, Vienna, Austria

4 Institute of Plant Biology, University of Zurich, Winterthurerstrasse 190, CH-8057, Zurich, Switzerland

5 Current address: Institute of Plant Biology, University of Zurich, Zollikerstrasse 107, CH-8008, Zurich, Switzerland

6 Current address: Institute of Microbiology, Ernst-Moritz-Arndt University of Greifswald, Friedrich-Ludwig-Jahn-Strasse 15, D-17487 Greifswald, Germany

7 Fungal Genetics and Genomics Unit, Department of Applied Genetics and Cell Biology, University of Natural Resources and Life Sciences, Konrad-Lorenz-Strasse 24, A-3430 Tulln, Austria

8 AIT Austrian Institute of Technology GmbH, Bioresources Unit, Konrad-Lorenz-Strasse 24, A-3430 Tulln, Austria

*** E-mail: Corresponding author@institute.edu**

Abstract

Lignin is a major component of plant litter and is considered highly resistant to decomposition. Carbohydrates, in contrast, are more easily degraded. We studied the decomposition rates of these two compound classes, and to which extent they are controlled by litter C:N:P stoichiometry.

Herein we report results from a 15-months mesocosm experiment under controlled climatic conditions with beech litter of different N and P contents. Litter was sterilized and re-inoculated prior to the experiment to minimize differences in the initial microbial community, but study the effect of N and P contents on identical initial decomposer communities. Lignin and carbohydrate decomposition rates were determined by pyrolysis-GC/MS for 2 periods (0-6 months and 6-15 months), the composition of the microbial community was monitored via metaproteome analysis.

Differences in litter nutrient contents led to the establishment of different decomposer communities. Fungi were dominant on all litter, but fungi:bacteria ratios were highest on high-nutrient litter, leading to a negative correlation between litter and microbial stoichiometry and high differences between litter and microbial C:N and C:P ratios on nutrient poor litter.

Rates of lignin decomposition were highly variable during the first six months, ranging from insignificant amounts decomposed to decomposition at bulk C mineralization rates. Between 6 and 15 months, lignin was degraded at bulk mass loss rates independent of the litter nutrient contents, however, different lignin contents acquired within the initial 6 months remained in place. Early lignin degradation rates were highest in litter with low fungi:bacteria ratios, and were correlated to differences between litter and microbial stoichiometry ($C:P_{litter:microbial}$ and $C:N_{litter:microbial}$). Lignin degrading communities were enriched in γ -proteobacteria after 6 months incubation.

Our results indicate that - contradicting common models - significant amounts of lignin were degraded during early decomposition in low nutrient litter. We demonstrate that litter quality profoundly affects the lignin decomposition via the composition of the decomposer community. Even though bacterial biomass is enriched in N and P, communities low nutrient litter were enriched in bacteria. This led to higher differences between litter and microbial stoichiometry, a possible control over lignin degradation during early decomposition.

Introduction

Plant litter is quantitatively dominated by macromolecular compounds. In foliar litter, lignin and carbohydrate polymers like cellulose together make up 40-60% of litter dry mass [?], while leachable substances account for only 1.5-6% [?]. The breakdown of high molecular weight compounds into smaller molecules that are accessible to microbes is mediated by extracellular enzymes and is considered to be rate limiting for decomposition [?].

Common models of litter decomposition [?, ?, ?, ?] assume that organic compounds in litter form up to three independent pools of increasing recalcitrance, i.e. (1) soluble compounds, (2) cellulose and hemicelluloses, and (3) lignin and waxes (cutin and suberin). Soluble compounds are most accessible to microbes and are usually consumed first, followed by regular polymers, such as cellulose. Lignin is not degraded until accumulated to a certain, critical level when it inhibits the degradation of less recalcitrant compounds. Most studies quantified these pools by gravimetric determination of the amount of cellulose, hemicelluloses and lignins after sequential extractions with selective solvents. These methods were repeatedly criticized for being unspecific for lignin determination [?]. When analyzed with alternative methods (NMR, CuO-oxidation, Pyrolysis-GC/MS), extracted lignin fractions were shown to contain also many other substances [?], which led to an overestimation of lignin accumulation during early decomposition [?].

Recent studies based on more specific methods to determine litter lignin contents question the intrinsic recalcitrance of lignin. Isotope labeling experiments with soils and litter/soil mixtures, undertaken both in-situ and under controlled conditions, revealed mean residence times of lignin in soils in the range of 10-50 years, much less than expected and shorter than that of bulk soil organic matter [?, ?, ?]. While the ability to completely degrade lignin was traditionally attributed exclusively to Basidiomycetes, it has been demonstrated for several bacterial taxa over the last years [?].

For leaf litter, lignin decomposition even at early stages of litter decay and lignin decomposition rates that decreased during decomposition were recently reported by Klotzbücher and colleagues [?]. They proposed that lignin decomposition is limited by labile C sources and that therefore fastest lignin degradation occurs during early litter decomposition.

Additionally, the decomposition of lignin may also be dependent on the nutrient content of the litter and thus the nutritional status of the microbial community. During radical polymerization, significant amounts of cellulose and protein are incorporated into lignin structures [?]. In isolated lignin fractions from fresh beech litter, N contents twice as high as in bulk litter were found [?]. It was therefore argued that, while

yielding little C and energy, lignin decomposition makes protein accessible to decomposers that is occluded in plant cell walls, and that lignin decomposition is therefore not driven by C but by the N demand of the microbial community ("Nitrogen mining theory", [?]). In favor of the N mining theory, fertilization experiments indicated N exerts an important control on lignin degradation: N addition increased mass loss rates in low-lignin litter while slowing down decomposition in lignin-rich litter [?] and decreased the activity of lignolytic enzymes in forest soils [?]. Incubation experiments with soil-litter mixtures showed that N fertilization led to a decrease in the mineralization of complex soil carbon, while no such effect was found after P fertilization [?]. This is explained because soil P is protected by inorganic mechanisms rather than incorporation into humic substances, however, no data is available whether this is also the case in decomposing plant litter.

It was recently been shown that addition of N has a different effect on litter decomposition than varying N levels in litter [?]. This is due to the fact that leaf litter N is stored in protein and lignin structures and not directly available to microorganisms, while fertilizer N is added in the form of readily available inorganic N (ammonium, nitrate or urea). A similar effect has to be expected for P. Fertilization experiments can thus simulate increased nutrient deposition but not the effect of litter nutrient contents on decomposition processes.

Our study therefore aimed at analyzing the effect of variations in beech litter nutrient (N and P) content on lignin and carbohydrate decomposition rates. Towards this end, we followed the breakdown of lignin and carbohydrates by pyrolysis-GC/MS (pyr-GC/MS) during a mesocosm experiment under constant environmental conditions over a period of 15 month. In order to exclude effects resulting from different initial microbial communities, we sterilized beech litter samples from 4 different locations in Austria and re-inoculated them prior to the experiment with an litter/top-soil inoculum from one of the sites. Additionally, we analyzed the microbial meta-proteome in a subset of our mesocosms to assess the activity of bacterial and fungal taxa.

With the experiment, we addressed the following questions:

(1) Is lignin decomposition delayed until late decomposition stages or are significant amounts of lignin already degraded during early litter decomposition, and does the timing of lignin decomposition depend on litter stoichiometry? We hypothesized, that lignin decomposition is initially slower in litter with a narrow C:N ratio (higher availability of assimilable nitrogen), than in litter with a high C:N ratio.

(2) Are high lignin degradation rates related to a higher fungal activity? We hypothesized that wider C:N and C:P ratios favor lignin degradation by fungi while narrow C:N and C:P ratios favor carbohydrateo

degradation by bacteria.

Results

Initial litter chemistry

Initial litter chemistry of the four sites (Achenkirch, AK, Klausenleopoldsdorf, KL, Ossiach, OS, Schottenwald, SW), measured 14 days after incubation, is presented in supplemental table ???. C:N ratios varied between 41:1 and 58:1 and C:P ratios between 700:1 and 1300:1, while N:P ratios ranged between 15:1 and 30:1. We found no significant changes of litter stoichiometry during the incubation except of the C:N ratio in the fastest degrading litter (SW), which slightly decreased after 15 months (41.8:1 to 37.4:1). Lignin and carbohydrate contents before incubation were in a similar range in all litter, lignin accounted for 28.9-31.2% and carbohydrates for 25.9-29.2% of the total peak area of all pyrolysis products. Micronutrient contents strongly varied: Fe concentrations were more than twice as high in OS (approx. 450 ppm) than for other litter (approx. 200 ppm), Mn contents were highly variable and ranged between 170 and 2130 ppm. All changes of micro-nutrient concentrations during incubation were <15% of the initial concentration.

Mass loss, respiration and soluble organic C, N and P

Highest respiration rates were measured at the first measurement after 14 days incubation (150-350 $\mu\text{g CO}_2\text{-C d}^{-1} \text{ g}^{-1} \text{ litter-C}$), which dropped to 75 to 100 $\mu\text{g CO}_2\text{-C d}^{-1} \text{ g}^{-1} \text{ litter-C}$ after 3 months. After 6 and 15 months, respiration rates for AK and OS further decreased, while SW and KL showed a second maximum in respiration after 6 months (fig ??).

Litter mass loss was not significant after 2 weeks and 3 months, and significant for 2 litter from two sites after 6 months. After 15 months, litter mass loss was significant for all collection sites, and ranged between 5 and 12 % of the initial dry mass, and was strongly correlated to litter N content ($R=0.794$, $p<0.001$). Detailed results were reported by [?]. Accumulated respiration was strongly correlated to litter mass loss after 15 months ($r=0.738$, $p<0.001$, $n=20$).

Soluble organic carbon concentrations decreased between the first three harvests (14 days to 6 months), and strongly increased to 15 months (from 0.1 to 0.7 $\text{mg C g}^{-1} \text{ d.w.}$ to 1.5 to 4 $\text{mg C g}^{-1} \text{ d.w.}$ after 15 months, fig. ??). After 14 days and 3 months, the highest soluble organic C concentrations were found in SW litter followed by AK. Soluble organic C concentrations were initially only weakly correlated

with litter N content after 14 days ($r=0.69$, $p<0.001$, $n=20$) and after 3 months ($r = 0.65$, $p<0.01$, $n=20$), but strictly correlated after 6 months ($r=0.85$, $p<0.001$, $n=20$) and 15 months ($r=0.90$, $p<0.001$, $n=20$), indicating an increasing independence on litter N contents. Soluble N (not shown) was tightly correlated to soluble organic C ($R=0.992$, $p <0.001$, $n=80$) with *Corg*:N ratios falling from initially 30:1-40:1 to 20:1-30:1. Soluble P contents ranged between 70 and 400 $\mu\text{g g}^{-1}$ d.w., and were highly correlated to litter P contents ($R=0.830$, $p <0.001$, $n=80$). Within the initial 6 month of incubation, soluble P decreased in high-P litter and increased in low-P litter (fig. ??).

Potential enzyme activities

Within each time point, all potential extracellular enzyme activities were correlated with litter N and actual respiration rates (all $R>0.8$, $p<0.001$, $n=20$). Cellulase activity increased from the first harvest onwards to 15 months, with a small depression after 6 months (Fig. ??), phenoloxidase and peroxidase activities reached their maximum between 3 and 6 months (fig. ??). For all enzymes and at all time points, SW showed the highest and AK the lowest activities. Differences between these two sites were more pronounced in cellulase activity (SW 10x higher than AK) than in oxidative enzymes (SW 4x higher). Conversely, the phenoloxidase/cellulase ratio was highest for AK and lowest for SW at all time points and decreased during litter decomposition (fig. ??).

Microbial biomass abundance and community composition

Microbial biomass contents ranged from 0.5 to 6 mg C g^{-1} d.w., 0.05 to 0.55 mg N g^{-1} d.w. and 0.05 to 0.35 mg P g^{-1} litter d.w (fig. ??). After an initial increase in microbial biomass, in KL and OS microbial biomass remained constant after 3 months while AK and SW showed further accumulation of microbial biomass which reaches a maximum of microbial C and N contents after 6 months (AK also for P). Microbial C:N ratios ranged between 6:1 and 18:1, C:P ratios between 8:1 and 35:1, and N:P ratios between 0.5:1 and 3.5:1 (fig. ??). The differences between microbial and litter stoichiometry led to an accumulation of substantial amounts of P (up to 80% of the total litter P in AK after 6 months). In AK and KL litter biomass P includes initially insoluble P that was mobilized (ie. the sum of soluble + biomass P contents increased), while in OS and SW litter and microbial P was taken up from a shrinking soluble P pool (fig. ??).

Microbial biomass was stoichiometrically homeostatic during the first 6 months (no or negative correlations between microbial C:N:P and litter C:N:P, see also [?]), but after 15 months (microbial C:N:P ratios

were significantly and positively correlated to resource stoichiometry: $R=0.53-0.64$, all $p<0.002$). The homeostatic regulation coefficients [?] were $H_{C:P}=1.68$, $H_{C:N}=2.01$, and $H_{N:P}=2.29$ after 15 month incubation. Microbial C:N ratios after 3 and 6 months were within a tightly constrained range, 14.5:1 to 18.2:1 after 3 months and 6.9:1 to 9.0:1 after 6 months, but significantly different between the two sampling events. In contrast, microbial C:P and N:P ratios were less constrained, with the highest variance between litter from different sites after 3 months of incubation (fig. ??).

Metaproteome analysis yielded between 451 and 1113 (average 639) assigned spectra per sample (one replicate per collection site after 14 days, 3, 6, and 15 months). For community profiling only spectra assigned to bacteria or fungi were used. Fungal proteins were dominant in all litter types at all stages, but most prominent in high-nutrient SW and least pronounced in low-nutrient AK litter. Fungi:bacteria (F:B) protein abundance ratios were highest after 14 days (5 to 12) and decreased during litter decomposition (1.7 to 3 after 15 months, see fig. ??). The large initial differences in F:B ratios between litter from different sites decreased during decomposition. In addition, F:B ratios were measured on a DNA basis (qPCR) the results showing a similar pattern but with a much larger fungal DNA dominance (F:B ratios between 10-180). F:B ratios were highly correlated between protein- and log-transformed DNA-based estimates ($r=0.785$, $p<0.001$, $n=20$).

Fungal communities were dominated by Ascomycota, with smaller contributions by Basidiomycota (<5% of fungal protein). Among the fungal classes found, Sordariomycetes and Eurotiomycetes were most abundant with further contributions of Dothideomycetes, Leothiomycetes and Saccharomycetes (fig. ??). Bacteria were dominated by Proteobacteria (mainly γ , declining, and α - and β -Proteobacteria, increasing with litter decomposition) with minor contribution of Actinomycetes and Bacterioidetes (both increasing) and Thermotogae (decreasing, fig. ??).

Pyrolysis-GC/MS and Lignin content

In total 128 pyrolysis products were detected, quantified, identified and assigned to their substances of origin (suppl. tab. 1). We found only minor changes in the relative concentration of litter pyrolysis products during decomposition, and differences between sites were small but well preserved during decomposition. However, the high precision and reproducibility of pyrolysis GC/MS analysis of litter allowed tracing small changes in lignin and carbohydrate abundance during decomposition. Lignin-derived compounds made up between 29 and 31 % relative peak area (TIC) in initial litter, and increased by up to 3 %. The increase occurred almost exclusively during the first 6 months. Carbohydrate-derived pyrolysis products accounted for 26 to 29 %

in initial litter and decreased by up to 2.6 % within 15 months of incubation. The initial (pyrolysis-based) lignin:carbohydrate indices (LCI) were highly similar between litter from different collection sites, ranging between 0.517 and 0.533 (Fig. 4). During decomposition, the LCI increased by up to 9 % of the initial value. The highest increase was found in SW litter, while LCI slightly decreased in AK litter. All significant changes in LCI occurred within the first 6 months (fig. ??). As differences in lignin and carbohydrate contents between 0-3 and 3-6 months were not significant, we analyzed differences for two time intervals, i.e. between 0-6 months and 6-15 months.

During the first 6 months, between one and 6 % of the initial lignin pool and between 4 and 17% of the initial carbohydrate pool were degraded (Fig. ??). Lignin decomposition was highest in AK and KL litter, while microbial communities of KL, OS and SW litter decomposed carbohydrates faster. Lignin preference values (% lignin decomposed : %carbohydrates decomposed) were lowest in SW and highest in AK litter (Figure 5). In AK litter, lignin macromolecules were 50 % more likely to be decomposed than carbohydrates, while in SW litter carbohydrates were 10 times more likely to be decomposed (fig. ??). Between 6 and 15 months, no further accumulation of lignin occurred. Lignin and carbohydrates were both degraded at the same rate and their relative concentrations remained constant between 6 and 15 months (fig. ??).

Correlations between lignin and carbohydrate decomposition and litter chemistry, microbial community and decomposition processes

To assess possible controls over lignin degradation, we tested relationships between lignin and carbohydrate degradation, litter chemistry, microbial biomass and decomposition processes after 6 and 15 months for correlations (tables ?? and ??) including data presented previously [?,?]. After the initial 6 months, when differences in lignin accumulation were highest, the ratio of lignin:cellulose degradation was positively correlated with the ratio of phenoloxidase : cellulase ($R=0.599$, $p=0.005$, $n=20$) and peroxidase : cellulase ($R=0.734$, $p<0.001$, $n=20$). In contrast, lignin decomposition was negatively correlated to litter P, but positively with litter C:P and N:P ratios. The best correlation of lignin : carbohydrates degradation rates and LCI were found with both $C:P_{litter:microbial}$ and $C:N_{litter:microbial}$ (fig. ??), however, these two ratios were also intercorrelated ($R=0.641$, $p=0.002$, $n=20$). In contrast, carbohydrate decomposition was positively correlated with litter N content, and negatively with litter C:N ratios and $C:N_{litter:microbial}$.

Between 6 and 15 months, the ratio of lignin : carbohydrate decomposition was no longer related to stoichiometry or elemental composition any more. During this later period, lignin and carbohydrate decom-

position exhibited the same controls, being positively correlated to soluble organic C, litter N and litter P (table ??) between 6 and 15 months. Mass loss and accumulated respiration were positively correlated to lignin and carbohydrate decomposition (table ??), a pattern that we did not find for lignin decomposition in the early decomposition phase (table ??). Protein abundance F:B ratios were negatively correlated to the ratios of lignin : cellulose decomposition and to LCI change during the first 6 months, pointing to bacterial engagement in lignin decomposition. In contrast, both lignin and carbohydrate decomposition rates, were positively correlated with F:B ratios after 15 months, pointing to fungal dominance of both lignin and carbohydrate decomposition. No correlation between F:B ratio and the ratio of lignin : cellulose decomposition was found in this later period (fig. ??).

To assess the interaction between litter chemistry, microbial community and degradation processes, we conducted a correspondence analysis (CA) of the metaproteome data (relative protein abundances, fig. ??). The results indicate that incubation time (i.e. succession) is the dominant factor controlling the microbial community, with samples collected at the first (14 days) and the last (15 month) sampling grouping closely together, while litter quality (i.e. elemental stoichiometry of litter collected at different sites) had a higher impact after 3 and 6 months. The first factor (CA 1), which explained 35.7 % of the total variance, separates litter sampled after 15 months (positive values) from litter sampled earlier (negative values). Consequently, CA 1 was also positively correlated to incubation time and negatively to litter C content (i.e. decreasing C:N ratios during decomposition). A number of bacterial taxa (Actinobacteri, Bacteroidetes, α - and β -proteobacteria), and two fungal classes (Leotiomycetes and Tremellomycetes) were positively correlated to CA1 i.e. increased in abundance towards 15 months, while Cyanobacteria, ϵ -proteobacteria and Saccharomycetes were negatively correlated. CA 2, which explained 26.0 % variance, separated litter sampled within the first 6 months. Dothideomycetes and Sordariomycetes were positively and γ -proteobacteria negatively correlated to this factor, which also correlated to the F:B protein abundance ratio. Litter collected 14 days after inoculation have the highest scores on CA 2, while sites with active lignin degradation within the first 6 months (AK, KL) have the most negative scores. The axis was furthermore correlated to the microbial biomass P content and $C:P_{litter:microbial}$ and $N:P_{litter:microbial}$. For samples analyzed after 6 months, where direct comparison to lignin degradation rates was possible, significant correlations to CA 2 were found for lignin : carbohydrate degradation ($r=-0.97$, $p=0.028$), % Lignin loss : % Carbon loss ($r=-0.96$, $p=0.040$) and LCI increase ($r=0.973$, $p=0.027$), even though the number of independent samples was very low ($n=4$). Differences in CA2 strongly decreased after 15 months, suggesting that the differences in the microbial community found within the first 6 months were diminished with succession of the decomposer

community. Litter N and P contents were not correlated to either factor, although differences in resource quality evidently affected community composition after 3 and 6 months, as can be seen in the differences in the microbial communities as observed in CA 2. Correlation of CA factors with litter stoichiometry, and microbial stoichiometry, and the abundance of the analyzed taxa are provided in supplemental table ??.

Discussion

Differences in litter qualities led to different mass loss rates and the development of different decomposer communities from the same inoculate. Lignin decomposition was highly variable between litter of different quality within the first 6 months; its decomposition ranged from non-detectable (SW litter) to decomposition at bulk carbon loss rates (ie. no lignin accumulation, AK litter). This provides further evidence that the use of extractive methods to measure lignin contents led to an underestimation of early lignin degradation rates, as recently suggested [?], and that substantial amounts of lignin can be degraded during early decomposition. In contrast, between 6 and 15 months, lignin was degraded at the same rate as bulk carbon in all litter, regardless of litter quality. During this time, the different lignin contents acquired within the first six months remained in place, but lignin contents no further increased.

We chose our collection sites to provide litter with different N and P contents since we focused on the effect of these nutrients on decomposition. We found positive correlations between litter N and bulk decomposition parameters like carbon mineralization rates and extracellular enzymatic activities, indicating litter decomposition was limited by litter N. No such correlation was found for litter P contents. However, AK litter, which had low contents in both N and P, had a lower C mineralization rate than KL and OS, which had lower contents of N or P, respectively, than AK, suggesting a co-limitation of both elements. The use of litter of a single species from different sites minimized differences in other litter traits, and eg. initial carbohydrate and lignin contents of all samples fell in a narrow range for litter from all sites. However, litter N and P contents are also proxies for other litter traits not directly measurable (e.g. leaf morphology), which resulted from the plant's response to nutrient availability (e.g. for low P adaptation see [?]). N and P were also demonstrated to be correlated to a wide area of leaf traits in plants (ie. [?]), and such leaf traits were successfully used to predict litter decomposability in the past [?].

The composition of the microbial community changed with both by time (i.e. succession) and collection site (i.e. litter quality). While all samples measured were dominated by fungi, fungi:bacteria ratios decreased over time and were higher in nutrient-rich litter than in nutrient-poor litter (SW ■AK). Our results con-

tradicted the often-cited predictions that higher N and P contents would favor bacterial over fungal growth because bacterial biomass has lower C:N and C:P ratios than fungal biomass [?]. In contrast, we found fungi : bacteria ratios were higher in nutrient-rich litter. Similar observations were reported by Güsewell and Gessner 2009, who suggested that bacteria compensate N deficiency by heterotrophic N fixation, and therefore colonize low-N litter more successfully. However, microbial decomposers excrete important amounts of N as extracellular enzymes, which further raise their N demand; a factor not represented in the biomass C:N ratios. The higher abundance of bacteria on low nutrient litter would also be explained if fungi produced more extracellular enzymes per biomass than bacteria, therefore have creating a more narrow C:N demand than bacteria even though their biomass has a wider C:N ratio. In result, bacteria-rich decomposers with more narrow C:N and C:P biomass developed on low-nutrient sites, with more narrow C:N and C:P ratios, further increasing difference between microbial and litter stoichiometry. To consider both litter and microbial stoichiometry, we used $C:X_{litter:microbial}$ ratios as integrated measure for nutrient availability to nutrient demand.

Litter quality controlled the composition of the microbial communities, and microbial biomass stoichiometry, which influenced the stoichiometric offset between resource (litter) and consumer (microbial biomass) that decomposers had to overcome. Both community composition, and $C:X_{litter:microbial}$ and were correlated to the rate of early lignin decomposition; Litter with high fungi:bacteria ratios and lower differences between litter and microbial stoichiometry accumulated more lignin. Our results therefore indicate that lignin degradation is associated with bacteria-rich degrader communities, a low availability of nutrients to decomposers, or both. In contrast, we can exclude that lignin decomposition was triggered by critical lignin contents or inhibited by insufficient Mn (highest lignolytic activity in litter with lowest contents of lignin and Mn), as suggested for late lignin decomposition [?].

Traditionally, the capability to completely degrade lignin was exclusively attributed to Basidiomycota fungi [?]. However, fungi:bacteria ratios were lower in lignin degrading litter and Basidiomycota produced less than 5% of fungal protein. Over the last years, lignin degradation was also demonstrated for several bacterial taxa (eg. actinomycetes, α -, and γ -proteobacteria [?]). Of these three taxa, we found one (γ -proteobacteria) correlated to lignolytic activities after 3 and 6 months. The other two taxa (actinomycetes and α -proteobacteria) were enriched after 15 months in all litter types, when lignin decomposition was found in litter from all sites (ie. independent from litter quality). However, the metaproteomic analysis only sporadically detected lignolytic enzymes, we can not attribute lignolytic activities to specific taxa at this time. Nevertheless, our data indicates that corresponding trends for lignin degradation and fungal :

bacterial protein abundance both along succession and between litter from different sites after 6 months (higher lignolytic activity at low fungi:bacteria ratios).

Lignin degradation in the first 6 months was best predicted by $C:P_{litter:microbial}$ and $C:N_{litter:microbial}$, ie. more lignin was degraded when the difference between litter and microbial stoichiometry was higher. $C:P_{litter:microbial}$ and $C:N_{litter:microbial}$ were intercorrelated, so we can not differentiate the effects of N and P. However, lignin decomposition rates were negatively correlated to litter P, but not N contents and positively correlated to microbial biomass P contents, while carbohydrate decomposition was positively correlated to litter N. This would indicating a differential control of lignin (stimulated by P demand) and carbohydrate (stimulated by N availability) decomposition. Litter which rapidly degraded lignin (AK and KL) net-mobilized insoluble P into rapidly cycled P forms (soluble and microbial), while in slowly lignin degrading litter (SW and OS) microbial P originated only from soluble P (fig. ??B). This indicates that lignin degradation increased the mobilization of P from insoluble litter biomass, and explains higher lignin degradation rates in litter with high microbial P demand. Such a nutrient mobilization by lignin degradation is assumed for N [?]: Lignin (like humic compounds) occludes important amounts of protein during polymerization [?,?], which is available only after lignin degradation. Therefore, the degradation of complex carbon sources was proposed to constitute a strategy of N sequestration (N mining theory, [?,?]). However, ambivalent results are reported for whether P is protected in lignin and humic compounds, and whether P demand triggers the decomposition of complex carbon compounds [?,?].

The degradation of lignin and carbohydrate polymers depends on the excretion of different extracellular enzymes. Their production is N intensive, therefore a trade-off exists between the production of cellulolytic and lignolytic enzymes [?]. Lignin decomposition was also suggested to allow decomposers direct competition by the early colonization of lignin rich sites [?]. We found higher activities of both cellulolytic and lignolytic enzymes in N-rich litter, but their ratio was well correlated to lignin : carbohydrate decomposition. Lignin degradation yields less C and energy than carbohydrates degradation, but might provides additional N. When $C:X_{substrate:consumer}$ is low, as it was the case for lignin degrading litter, additional carbon can not be used by decomposers to build up biomass. Therefore, the observed increase in lignolytic activities might result from a microbial strategy to optimize N allocation between cellulolytic and lignolytic enzyme systems when additional C can not be utilized by the decomposer due to a lack of nutrients.

In summary, litter quality exercised a profound control on the litter decomposition process, including community composition and lignin accumulation. Lignin decomposition within the first six months was highly variable between litter of the same species but different in nutrient contents, and ranged from no

lignin degradation to lignin degradation at bulk litter C loss rates. Lignin decomposition was not coupled to fungi-rich decomposer communities, indicating important bacterial contributions to lignin decomposition. Early lignin decomposing litter was characterized by nutrient-rich microbial biomass on low-nutrient litter, ie. a high difference between litter and decomposer stoichiometry, low fungi:bacteria ratios and an elevated abundance of γ -proteobacteria peptides. Different lignin contents acquired during early decomposition remained in place, potentially affecting late decomposition and humification.

Material and methods

Litter decomposition experiment

Beech litter was collected at four different sites in Austria (Achenkirch (AK), Klausenleopoldsdorf (KL), Ossiach (OS), and Schottenwald (SW); referred to as litter types) in October 2008. Litter was cut to pieces of approximately 0.25cm², homogenized, sterilized twice by γ -radiation (35 kGy, 7 days between irradiations) and inoculated (1.5% w/w) with a mixture of litter and soil to assure that all litter types share the same initial microbial community. From each type, four samples of litter were taken immediately after inoculation, dried and stored at room temperature. Batches of 60g litter (fresh weight) were incubated at 15 °C and 60% relative water content in mesocosms for 15 months. For each litter type 5 replicates were removed and analyzed after 14, 97, 181 and 475 days. A detailed description of the litter decomposition experiment was published by [?].

Bulk litter, extractable, and microbial biomass nutrient content

To calculate litter mass loss, litter dry mass content was measurement in 5 g litter (fresh weight) after 48 h at 80 °C. Dried litter was ball-milled for further chemical analysis. Litter C and N content was determined using an elemental analyzer (Leco CN2000, Leco Corp., St. Joseph, MI, USA). Litter phosphorus content was measured with ICP-AES (Vista-Pro, Varian, Darmstadt, Germany) after acid digestion [?]. To determine dissolved organic C, dissolved N and P, 1.8 g litter (fresh weight) were extracted with 50 ml 0.5 M K₂SO₄. Samples were shaken on a reciprocal shaker with the extractant for 30 minutes, filtered through ash-free cellulose filters and frozen at -20 °C until analysis. To quantify microbial biomass C, N and P, further samples were additionally extracted under the same conditions after chloroform fumigation for 24 h [?]. Microbial biomass was determined as the difference between fumigated and non-fumigated extractions .

C and N concentration in extracts were determined with a TOC/TN analyzer (TOC-VCPH and TNM, Shimadzu), P was determined photometrically as inorganic P after persulfate digestion [?].

Substrate to consumer stoichiometric imbalances $C:X_{substrate:consumer}$ were calculated as

$$C : X_{s:c} = \frac{C : X_{litter}}{C : X_{microbial}} \quad (1)$$

where X stand for the element N or P.

Microbial Respiration

Respiration was monitored weekly during the entire incubation in mesocosms removed after 6 month and on the last incubation day for all mesocosms using an infrared gas analyzer (IRGA, EGM4 with SRC1, PPSystems, USA). CO₂ concentration was measured over 70 seconds and increase per second was calculated based on initial dry mass. Accumulated respiration after 6 month was calculated assuming linear transition between measurements, accumulated respiration after 15 month was estimated from respiration rates after 181 and 475 days.

Potential enzyme activities

Potential activities of β -1,4-cellobiosidase (“cellulase”), phenoloxidase and peroxidase were measured immediately after sampling. 1 g of litter (fresh weight) was suspended in sodium acetate buffer (pH 5.5) and ultrasonicated. To determine cellulase activity, 200 μ l suspension were mixed with 25 nmol 4-methylumbelliferyl- β -D-cellobioside (dissolved in 50 μ l of the same buffer) in black microtiter plates and incubated for 140 min in the dark. The amount of methylumbelliferyl (MUF) set free in by the enzymatic reaction was measured fluorimetrically (Tecan Infinite M200, excitation at 365 nm, detection at 450 nm). To measure phenoloxidase and peroxidase activity litter suspension was mixed 1:1 with a solution of L-3,4-dihydroxyphenylalanine (DOPA) to a final concentration of 10 mM. Samples were incubated in microtiter plates for 20h to determine phenoloxidase activity. For peroxidase activity, 1 nmol of H_2O_2 was added before incubation. Absorption at 450 nm was measured before and after incubation. All enzyme activities were measured in three analytical replicates. The assay is described in detail in [?].

Pyrolysis-GC/MS

Pyrolysis-GC/MS was performed with a Pyroprobe 5250 pyrolysis system (CDS Analytical) coupled to a Thermo Trace gas chromatograph and a DSQ II MS detector (both Thermo Scientific) equipped with a carbowax column (Supelcowax 10, Sigma-Aldrich). Between 2-300 µg of dried and finely ground litter (MM2000 ball mill, Retsch) was heated to 600 °C for 10 seconds in a helium atmosphere. GC oven temperature was constant at 50 °C for 2 minutes, followed by an increase of 7 °C/min to a final temperature of 260 °C, which was held for 15 minutes. The MS detector was set for electron ionization at 70 eV in the scanning mode (m/z 20 to 300).

Peaks were assignment was based on NIST 05 MS library after comparison with measured reference materials. 128 peaks were identified and selected for integration either because of their abundance or diagnostic value. This included 28 lignin and 45 carbohydrate derived substances. The pyrolysis products used are stated in supplementary tables nn-nn¹ For each peak between one and four dominant and specific mass fragments were selected, integrated and converted to TIC peak areas by multiplication with a MS response coefficient [?, ?]. Peak areas are stated as % of the sum of all integrated peaks.

A pyrolysis-based lignin to carbohydrate index (*LCI*) was calculated to derive a ratio between these two substance classes without influences of changes in the abundance of other compounds .

$$LCI = \frac{Lignin}{Lignin + Carbohydrates} \quad (2)$$

Accounting for carbon loss, we estimate the % lignin and cellulose degraded during decomposition (L_{degr} and Ch_{degr}) according to equation ??, where X_{init} and X_{act} stand for initial and actual %TIC area of lignin or cellulose pyrolysis products, C_{init} for the initial amount of C and R_{acc} for the accumulated CO₂-C respired by a mesocosm.

$$X_{\%loss} = \frac{100}{X_{init}} \cdot \left(X_{init} - X_{act} \cdot \frac{(1 - R_{acc})}{C_{init}} \right) \quad (3)$$

Furthermore, we calculated the % of initial lignin or carbohydrates degraded per % of initial carbon respired (L:C_{degr} and Ch:C_{degr}):

$$X_{resp} = \frac{X_{\%loss}}{100} \cdot \frac{C_{init}}{R_{acc}} \quad (4)$$

¹check numbers!

Metaproteome analysis and quantitative PCR

From each harvest (14, 97, 181, and 475 days), one replicate per litter type was stored at -80°C for metaproteome analysis. 3 g of each sample were grounded in liquid nitrogen and extracted with Tris/KOH buffer (pH 7.0) containing 1% SDS. Samples were sonicated for 2 min, boiled for 20 min and shaken at 4 °C for 1 h. Extracts were centrifuged twice to remove debris and concentrated by vacuum-centrifugation. An aliquot of the sample was applied to a 1D-SDS-PAGE and subjected to in-gel tryptic digestion. The resulting peptide mixtures were analyzed on a hybrid LTQ-Orbitrap MS (Thermo Fisher Scientific) as described earlier [?]. Protein database search against the UniRef 100 database, which also comprised the translated metagenome of the microbial community of a Minnesota farm silage soil [?] and known contaminants, was performed using the MASCOT Search Engine. A detailed description of the extraction procedure and search criteria was published by [?]. If more than one protein was identified based on the same set of spectra these proteins were grouped together resulting in one protein cluster. The obtained protein/protein cluster hits were assigned to phylogenetic and functional groups and assignments were validated by the PROPHANE workflow (<http://prophane.svn.sourceforge.net/viewvc/prophane/trunk/>; [?]). Higher protein abundance is represented by a higher number of MS/MS spectra acquired from peptides of the respective protein. Thus, protein abundances were calculated based on the normalised spectral abundance factor (NSAF) [?, ?]. This number allows relative comparison of protein abundances over different samples [?]. Protein abundances were aggregated at class level for fungi and proteobacteria and at phylum level for other bacterial taxa. These abundances were subjected to a canonical correspondence analysis without constraints. Vectorial fittings of stoichiometrical ratios (litter, microbial biomass and imbalance) were calculated and plotted when $p < 0.05$.

Quantitative PCR was used to determine fungal and bacterial abundance as described recently [?]. F:B ratios were calculated as the ratio between estimated amounts of bacterial and fungal DNA found.

Statistical analysis

All statistical analyses were performed with the software and statistical computing environment R [?]. If not mentioned otherwise, results were considered significant when $p < 0.05$. Due to frequent variance inhomogeneities Welch ANOVA and paired Welch's t-tests with Bonferroni corrected p limits were used. All correlations mentioned refer to Pearson correlations. A correspondence analysis (CA) and vectorial fittings were calculated using the R package "vegan" [?].

Acknowledgments

This study formed part of the national research network MICDIF (Linking microbial diversity and functions across scales and ecosystems, S-10007-B01, -B06 and -B07) by the Austrian Research Fund (FWF). Katharina Keiblinger is a recipient of a DOC-ffORTE fellowship of the Austrian Academy of Sciences. Vital support regarding Pyr-GC/MS measurements was given by Clemens Schwarzingner, Andreas Blöchl and Birgit Wild.

References

1. Berg, B & McClaugherty C (2008) Plant Litter. Decomposition, Humus Formation, Carbon Sequestration. Berlin: Springer.
2. Don A, Kalbitz K (2005) Amounts and degradability of dissolved organic carbon from foliar litter at different decomposition stages. *Soil Biology and Biochemistry* 37: 2171–2179.
3. Sinsabaugh RL (2010) Phenol oxidase, peroxidase and organic matter dynamics of soil. *Soil Biology and Biochemistry* 42: 391–404.
4. Berg B, Staaf H (1980) Decomposition rate and chemical changes of Scots pine needle litter. II. Influence of chemical composition. *Ecological Bulletins* : 373–390.
5. Coûteaux MM, Bottner P, Berg B (1995) Litter decomposition, climate and litter quality. *Trends in ecology & evolution* 10: 63–66.
6. Moorhead DL, Sinsabaugh RL (2006) A theoretical model of litter decay and microbial interaction. *Ecological Monographs* 76: 151–174.
7. Adair EC, Parton WJ, Del Grosso SJ, Silver WL, Harmon ME, et al. (2008) Simple three-pool model accurately describes patterns of long-term litter decomposition in diverse climates. *Global Change Biology* : 2636–2660.
8. Hatfield RD, Romualdo SF (2005) Can Lignin Be Accurately Measured? *Crop Science* 45: 832–839.
9. Preston CM, Trofymow JA, Sayer BG, Niu J (1997) ^{13}C nuclear magnetic resonance spectroscopy with cross-polarization and magic-angle spinning investigation of the proximate analysis fractions used to assess litter quality in decomposition studies. *Canadian Journal of Botany* 75: 1601–1613.

10. Klotzbücher T, Filley TR, Kaiser K, Kalbitz K (2011) A study of lignin degradation in leaf and needle litter using ^{13}C -labelled tetramethylammonium hydroxide (TMAH) thermochemolysis: Comparison with CuO oxidation and van Soest methods. *Organic Geochemistry* 42: 1271–1278.
11. Amelung W, Brodowski S, Sandhage-Hofmann A, Bol R (2008) Combining Biomarker with Stable Isotope Analyses for Assessing the Transformation and Turnover of Soil Organic Matter. *Advances in Agronomy* 100: 155–250.
12. Thevenot M, Dignac MF, Rumpel C (2010) Fate of lignins in soils: A review. *Soil Biology and Biochemistry* 42: 1200–1211.
13. Bol R, Poirier N, Balesdent J, Gleixner G (2009) Molecular turnover time of soil organic matter in particle - size fractions of an arable soil. *Rapid Communications in Mass Spectrometry* 23: 2551–2558.
14. Bugg TD, Ahmad M, Hardiman EM, Singh R (2011) The emerging role for bacteria in lignin degradation and bio-product formation. *Current opinion in biotechnology* 22: 394–400.
15. Klotzbücher T, Kaiser K, Guggenberger G, Gatzek C, Kalbitz K (2011) A new conceptual model for the fate of lignin in decomposing plant litter. *America* 92: 1052–1062.
16. Achyuthan KE, Achyuthan AM, Adams PD, Dirk SM, Harper JC, et al. (2010) Supramolecular self-assembled chaos: polyphenolic lignin's barrier to cost-effective lignocellulosic biofuels. *Molecules (Basel, Switzerland)* 15: 8641–88.
17. Dyckmans J, Flessa H, Brinkmann K, Mai C, Polle A (2002) Carbon and nitrogen dynamics in acid detergent fibre lignins of beech (*Fagus sylvatica* L.) during the growth phase. *Plant, Cell & Environment* 25: 469–478.
18. Craine JM, Morrow C, Fierer N (2007) Microbial nitrogen limitation increases decomposition. *Ecology* 88: 2105–13.
19. Knorr M, Frey S, Curtis P (2005) Nitrogen addition and litter decomposition : A meta-analysis. *Ecology* 86: 3252–3257.
20. Talbot JM, Yelle DJ, Nowick J, Treseder KK (2011) Litter decay rates are determined by lignin chemistry. *Biogeochemistry* : 1–17–17.

21. Mooshammer M, Wanek W, Schnecker J, Wild B, Leitner S, et al. (2011) Stoichiometric controls of nitrogen and phosphorus cycling in decomposing beech leaf litter. Ecology in press.
22. Sterner RW, Elser JJ (2002) Ecological Stoichiometry. Princeton: Princeton University Press, 439 pp.

KEY: Sterner2002

ANNOTATION: From Duplicate 1 (Ecological stoichiometry: the biology of elements from molecules to the biosphere - Sterner, Robert Warner; Elser, James J.)

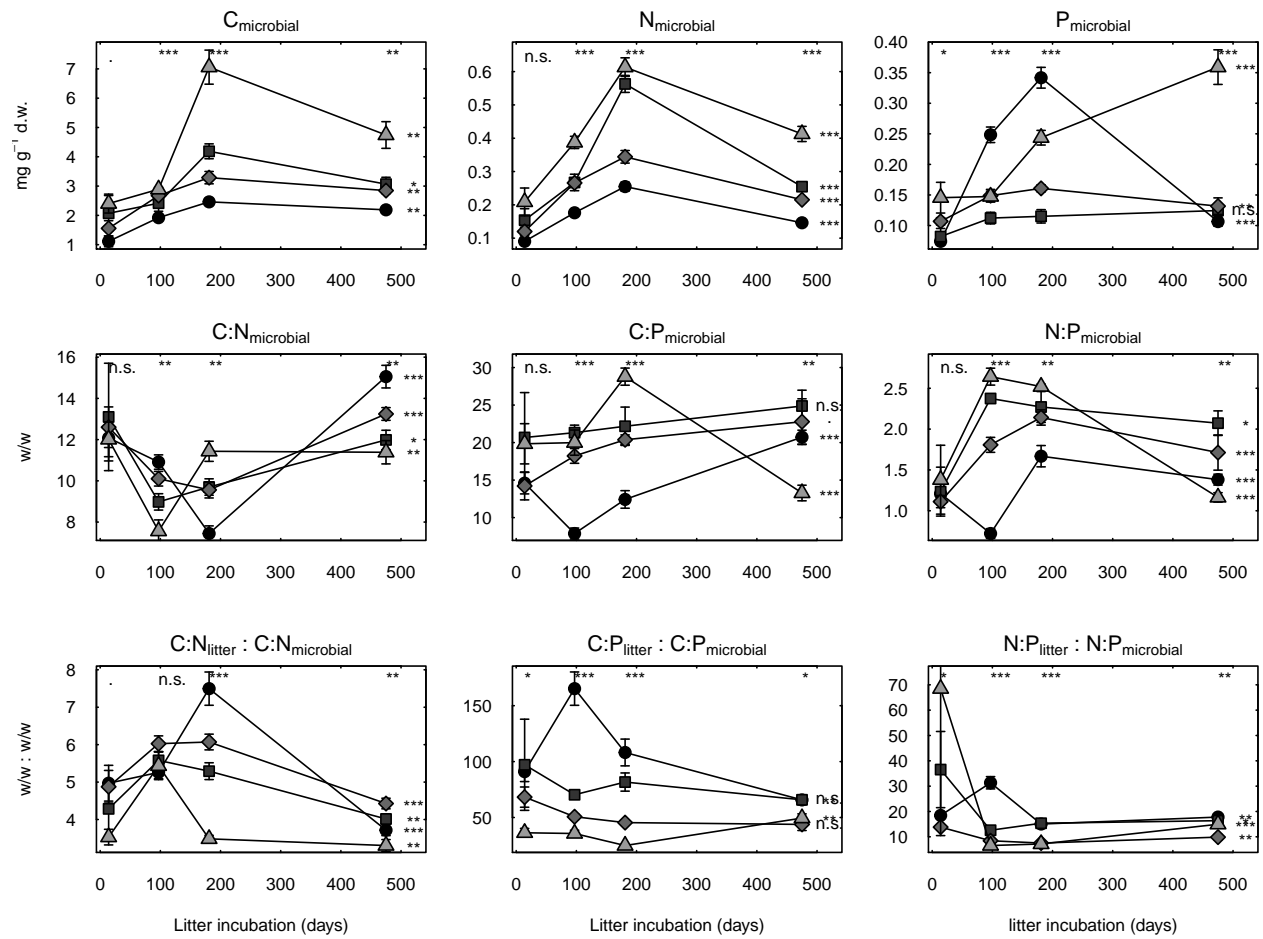
23. Leitner S, Wanek W, Wild B, Haemmerle I, Kohl L, et al. (2011) Linking resource quality to decomposition processes: Influence of litter chemistry and stoichiometry on glucan depolymerization during decomposition of beech (*Fagus silvatica* L.) litter. Soil Biology and Biochemistry in review.
24. Vance CP, Uhde-Stone C, Allen DL (2003) Phosphorus acquisition and use: critical adaptations by plants for securing a nonrenewable resource. New Phytologist 157.
25. Wright IJ, Reich PB, Cornelissen JHC, Falster DS, Garnier E, et al. (2005) Assessing the generality of global leaf trait relationships. The New phytologist 166: 485–96.
26. Cornelissen J, Thompson K (1997) Functional leaf attributes predict litter decomposition rate in herbaceous plants. New Phytologist 135: 109–114.
27. Hodge A, Robinson D, Fitter A (2000) Are microorganisms more effective than plants at competing for nitrogen? Trends in plant science 5: 304–8.
28. Treseder KK, Kivlin SN, Hawkes CV (2011) Evolutionary trade-offs among decomposers determine responses to nitrogen enrichment. Ecology letters .
29. Wanek W, Mooshammer M, Blöchl A, Hanreich A, Keiblinger K, et al. (2010) Determination of gross rates of amino acid production and immobilization in decomposing leaf litter by a novel N-15 isotope pool dilution technique. Soil Biology and Biochemistry 42: 1293–1302.
30. Kolmer J, Spaulding E, Robinson H (1951) Approved Laboratory Techniques. New York: Appleton Century Crafts.
31. Brooks P, Kragt J, Powlson D, Jenkinson D (1985) Chloroform fumigation and the release of soil nitrogen: the effects of fumigation time and temperature. Soil Biology & Biochemistry 17: 831–835.

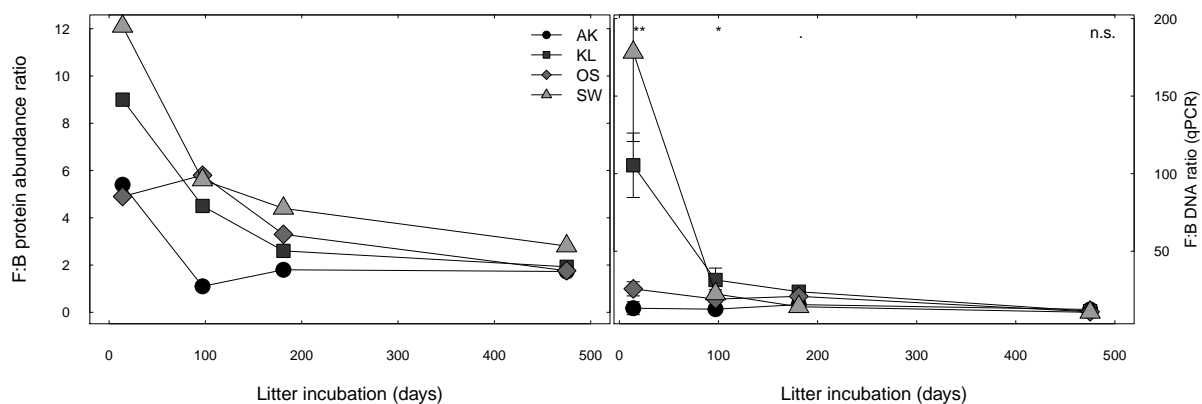
32. Schinner F, Öhlinger R, Kandeler E, Margesin R (1996) *Methods in Soil Biology*. Berlin: Springer Verlag, pp. 389 pp.
33. Kaiser C, Koranda M, Kitzler B, Fuchslueger L, Schnecker J, et al. (2010) Belowground carbon allocation by trees drives seasonal patterns of extracellular enzyme activities by altering microbial community composition in a beech forest soil. *New Phytologist* 187: 843–858.
34. Schellekens J, Buurman P, Pontevedra-Pombal X (2009) Selecting parameters for the environmental interpretation of peat molecular chemistry – A pyrolysis-GC/MS study. *Organic Geochemistry* 40: 678–691.
35. Kuder T, Kruege MA (1998) Preservation of biomolecules in sub-fossil plants from raised peat bogs - a potential paleoenvironmental proxy. *Organic Geochemistry* 29: 1355–1368.
36. Schneider T, Gerrits B, Gassmann R, Schmid E, Gessner MO, et al. (2010) Proteome analysis of fungal and bacterial involvement in leaf litter decomposition. *Proteomics* 10: 1819–30.
37. Tringe SG, von Mering C, Kobayashi A, Salamov Aa, Chen K, et al. (2005) Comparative metagenomics of microbial communities. *Science (New York, NY)* 308: 554–7.
38. Keiblinger KM, Schneider T, Roschitzki B, Schmid E, Eberl L, et al. (2011) Effects of stoichiometry and temperature perturbations on beech litter decomposition, enzyme activities and protein expression. *Biogeosciences Discussions* 8: 11827–11861.
39. Schneider T, Schmid E, de Castro JaV, Cardinale M, Eberl L, et al. (2011) Structure and function of the symbiosis partners of the lung lichen (*Lobaria pulmonaria* L. Hoffm.) analyzed by metaproteomics. *Proteomics* : 2752–2756.
40. Florens L, Carozza MJ, Swanson SK, Fournier M, Coleman MK, et al. (2006) Analyzing chromatin remodeling complexes using shotgun proteomics and normalized spectral abundance factors. *Methods (San Diego, Calif)* 40: 303–11.
41. Zybaylov B, Mosley AL, Sardi ME, Coleman MK, Florens L, et al. (2006) Statistical analysis of membrane proteome expression changes in *Saccharomyces cerevisiae*. *Journal of proteome research* 5: 2339–47.

KEY: Zybaïlov2006

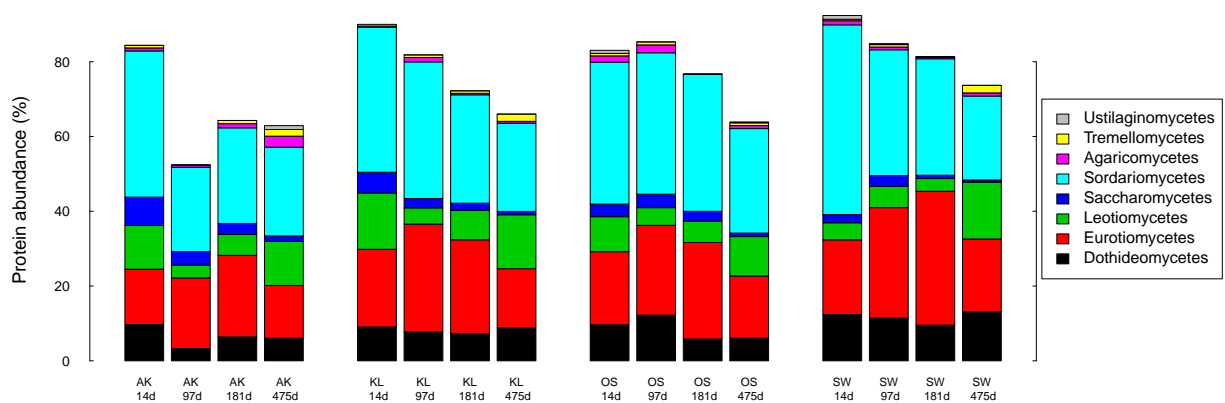
ANNOTATION: From Duplicate 1 (Statistical analysis of membrane proteome expression changes in *Saccharomyces cerevisiae*. - Zybaïlov, Boris; Mosley, Amber L; Sardiù, Mihaela E; Coleman, Michael K; Florens, Laurence; Washburn, Michael P)

42. Bantscheff M, Schirle M, Sweetman G, Rick J, Kuster B (2007) Quantitative mass spectrometry in proteomics: a critical review. *Analytical and bioanalytical chemistry* 389: 1017–31.
43. Inselsbacher E, Hinko-Najera Umana N, Stange FC, Gorfer M, Schüller E, et al. (2010) Short-term competition between crop plants and soil microbes for inorganic N fertilizer. *Soil Biology and Biochemistry* 42: 360–372.
44. R Development Core Team (2008). R: A Language and Environment for Statistical Computing. URL <http://www.r-project.org>.
45. Oksanen J, Blanchet FG, Kindt R, Legendre P, O'Hara R, et al. (2011). *vegan: Community Ecology Package*. R package version 1.17-9. URL <http://cran.r-project.org/package=vegan>.

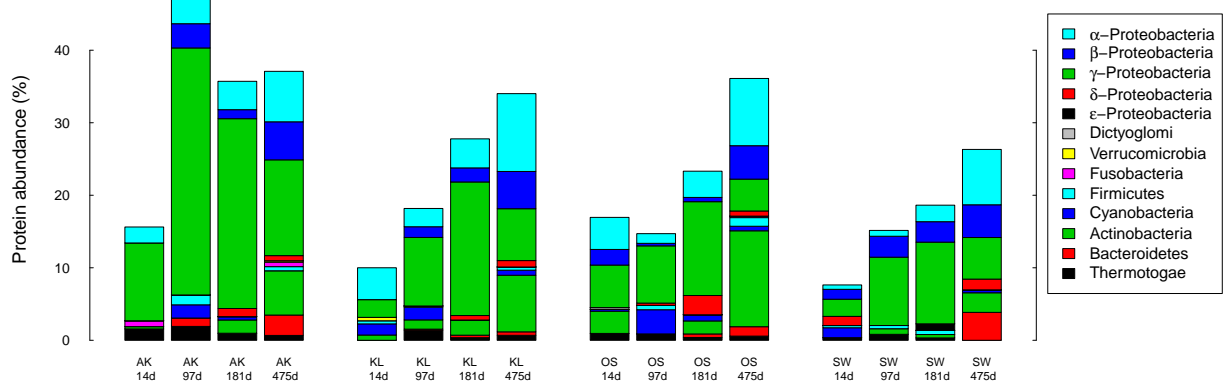


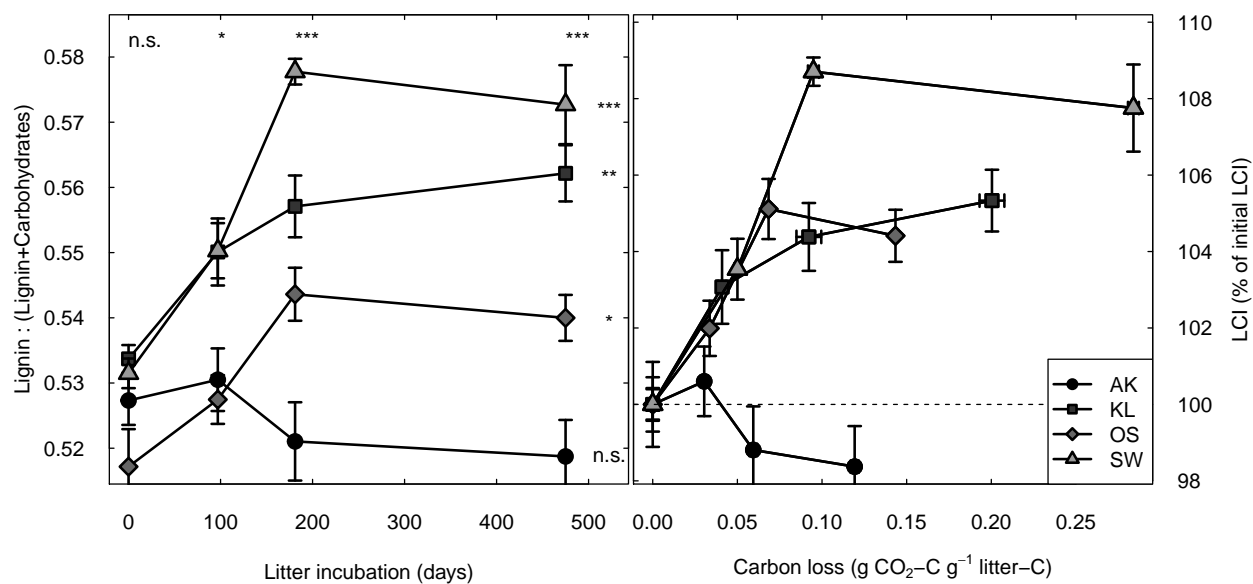
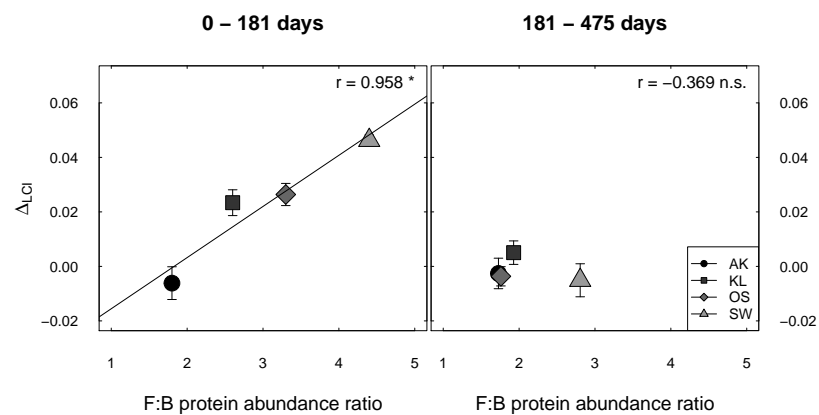


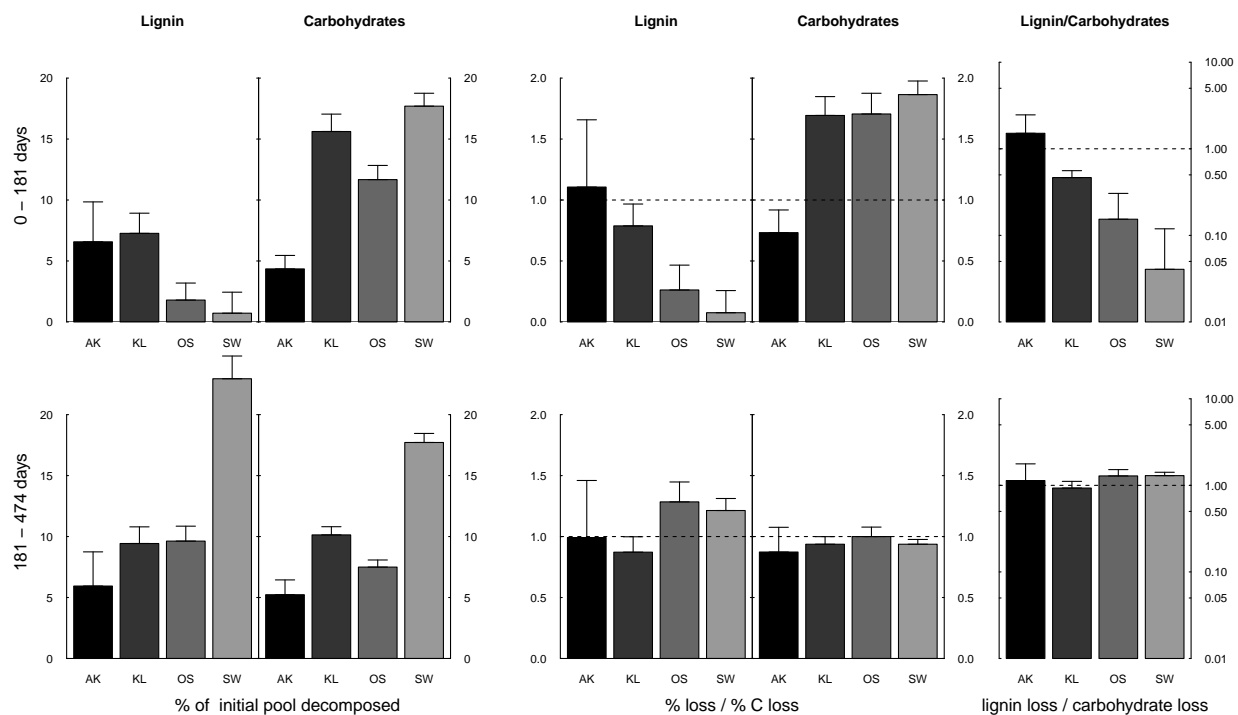
Fungal community



Bacterial community







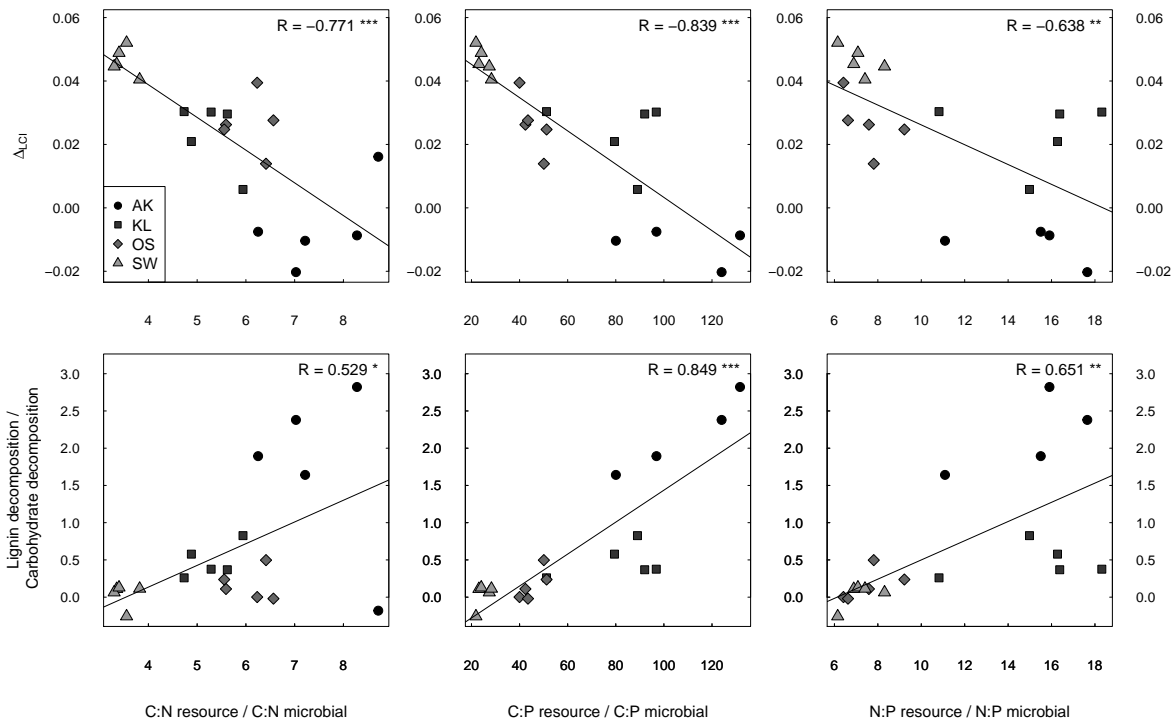


Table 1. Lignin derived and other phenolic pyrolysis products

Name	RT	MW	integrated fragments	Origin	Class
Guaiacol	18.87	124	109+124	Lignin	Guaiacyl
Methylguaiacol	20.32	138	123+138	Lignin	Guaiacyl
Ethylguaiacol	21.40	152	137+152	Lignin	Guaiacyl
Propenylguaiacol	23.29	164	149+164	Lignin	Guaiacyl
Vinylguaiacol	23.69	150	135+150	Lignin	Guaiacyl
Propenylguaiacol	24.48	164	149+164	Lignin	Guaiacyl
Syringol	24.58	154	139+154	Lignin	Syringyl
Propenylguaiacol	25.66	164	149+164	Lignin	Guaiacyl
Methylsyringol	25.67	168	153+168	Lignin	Syringyl
Ethylsyringol	26.39	182	167+182	Lignin	Syringyl
Propenylsyringol	27.97	194	179+194	Lignin	Syringyl
Vinylsyringol	28.37	180	165+180	Lignin	Syringyl
Guaiacolaldehyde	28.40	152	109+152	Lignin	Guaiacyl
Propylguaiacol	28.72	166	137+166	Lignin	Guaiacyl
Oxo-hydroxy-ethylguaiacol	28.77	182	182	Lignin	Guaiacyl
Propenylsyringol	28.91	194	179+194	Lignin	Syringyl
Oxo-ethylguaiacol	29.20	166	151+166	Lignin	Guaiacyl
Oxo-propylguaiacol	29.36	180	137+180	Lignin	Guaiacyl
Propenylsyringol	30.16	194	194+179	Lignin	Syringyl
Syringolaldehyde	32.68	182	139+182	Lignin	Syringyl
Oxo-hydroxy-ethylsyringol	32.80	212	212	Lignin	Syringyl
Guaiacolacetic acid	32.88	182	137+182	Lignin	Guaiacyl
Propylsyringol	33.15	196	181+196	Lignin	Syringyl
Oxo-propylsyringol	33.32	210	167+210	Lignin	Syringyl
Oxopropenylguaiacol	35.30	178	135+178	Lignin	Guaiacyl
Hydroxypropenylguaiacol	37.10	180	137+180	Lignin	Guaiacyl
Syringolacetic acid	38.78	212	212	Lignin	Syringyl
Oxo-propenylsyringol	43.06	208	165+208	Lignin	Syringyl
Phenol	21.02	94	65+66+94	Phenolic	
4-Methylphenol	22.11	108	107+108	Phenolic	
3-Methylphenol	22.22	108	107+108	Phenolic	
Ethylphenol	23.38	122	107+122	Phenolic	
Propenylphenol	26.93	134	133+134	Phenolic	
Propenylphenol	27.76	134	133+134	Phenolic	
Propylphenol	31.11	136	151+166	Phenolic	
Butylphenol	31.86	150	107+150	Phenolic	
4-Hydroxybenzaldehyde	32.70	122	121+122	Phenolic	
Hydroquinone	33.40	110	81+110	Phenolic	

Table 2. Carbohydrate derived pyrolysis products

Name	RT	MW	integrated fragments	Origin	Class
Acetaldehyde	2.06	44	29+44	Carbohydrates	
Furan	2.35	68	39+68	Carbohydrates	Furan
Methylfuran	2.74	82	81+82	Carbohydrates	Furan
Methylfuran	2.91	82	81+82	Carbohydrates	Furan
Dimethylfuran	3.43	96	95+96	Carbohydrates	Furan
Dimethylfuran	3.66	96	95+96	Carbohydrates	Furan
Vinylfuran	5.01	94	65+94	Carbohydrates	Furan
Unknown furan	6.36	108	107+108	Carbohydrates	Furan
Cyclopentanone	6.99	105	84+105	Carbohydrates	Cyclopentenone
Methylfuran	7.62	82	53+82+83	Carbohydrates	Furan
2-Oxopropanoic acid, methylester	7.92	102	43+102	Carbohydrates	
1-Hydroxypropanone	9.24	74	43	Carbohydrates	
2-Cyclopenten-1-one	10.26	82	53+54+52	Carbohydrates	Cyclopentenone
2-Methyl-2-cyclopenten-1-one	10.51	96	53+96	Carbohydrates	Cyclopentenone
1-Hydroxy-2-propanone	10.69	88	57+88	Carbohydrates	Cyclopentenone
Unknown	11.38	unk	65+66+94	Carbohydrates	
3-Furaldehyd	11.57	96	95+96	Carbohydrates	Furan
2(5H)Furanon	11.69	98	55+98	Carbohydrates	Furan
Propanoic acid, methylester	12.10	102	43+102	Carbohydrates	
2-Furaldehyd	12.22	96	95+96	Carbohydrates	Furan
Acetylfuran	12.99	110	95+110	Carbohydrates	Cyclopentenone
3-Methyl-cyclopentanone	13.31	96	67+96	Carbohydrates	Cyclopentenone
Dimethylcyclopentenone	13.69	110	67+95+110	Carbohydrates	Cyclopentenone
5-Methyl-2-furancarboxaldehyde	14.23	110	109+110	Carbohydrates	Furan
2-Cyclopenten-1,4-dione	14.44	96	54+68+96	Carbohydrates	Cyclopentenone
Butyrolactone	15.22	86	56+86	Carbohydrates	
Unknown	15.56			Carbohydrates	
Furanmethanol	15.61	98	98	Carbohydrates	Cyclopentenone
5-Methyl-2(5H)-furanone	16.06	98	55+98	Carbohydrates	Furan
Unknown	16.17	unk	110	Carbohydrates	
1,2-Cylopentandione	17.51	98	55+98	Carbohydrates	Cyclopentenone
Unknown	17.67	unk	42+70	Carbohydrates	
2-Hydroxy-3-methyl-2-cyclopenten-1-one	18.14	98	98	Carbohydrates	Cyclopentenone
3-Methy-1,2-cyclopentanedione	18.42	112	69+112	Carbohydrates	Cyclopentenone
Unknown	19.06		58+86+114	Carbohydrates	
Unknown	19.35		98+126	Carbohydrates	
Unknown	21.77		116	Carbohydrates	
Unknown	22.33		44	Carbohydrates	
Unknown	26.18		57+69	Carbohydrates	
5-Hydroxymethylfuran-1-carboxaldehyde	27.51	126	97+126	Carbohydrates	Furan
Unknown	31.67		73+135	Carbohydrates	
Laevoglucosan	40.44	172	60+73	Carbohydrates	

Table 3. Other pyrolysis products

Name	RT	MW	integrated fragments	Origin	Class
25:0 Alkan	27.74	352	57+71	aliphatic	Alkan
25:1 Alken	28.34	350	57+69	aliphatic	Alken
27:0 Alkan	30.04	380	57+67	aliphatic	Alkan
27:1 Alken	30.63	378	57+65	aliphatic	Alken
29:0 Alkan	32.20	408	57+63	aliphatic	Alkan
29:1 Alken	32.82	406	57+61	aliphatic	Alken
Myristic acid (14:0)	2.35	68	39+68	Lipid	Fatty Acid
Palmitic acid (16:0)	2.74	82	81+82	Lipid	Fatty Acid
Stearic acid (18:0)	2.91	82	81+82	Lipid	Fatty Acid
N-methyl-pyrrol	6.15	81	80+81	Protein	Pyrrol
Pyridine	6.90	95	52+79+95	Protein	Pyridine
Methylpyridine	7.50	93	66+92+93	Protein	Pyridine
Methylpyridine	7.54	93	66+92+93	Protein	Pyridine
methylpyridine	9.02	93	66+93	Protein	Pyridine
Pyrrol	13.11	67	39+41+67	Protein	Pyrrol
Methylpyrrol	13.81	81	80+81	Protein	Pyrrol
Methylpyrrol	14.10	81	80+81	Protein	Pyrrol
3-Hydroxypyridine	26.52	95	67+95	Protein	Pyridine
Indole	26.85	117	89+117	Protein	Indole
Methylindole	27.42	131	130+131	Protein	Indole
Toluene	4.54	92	91+92		Aromatic
Xylene	5.94	106	91+105+106		Aromatic
Xylene	6.09	106	91+105+106		Aromatic
Xylene	6.20	106	91+105+106		Aromatic
Xylene	6.99	105?	84+105?		Aromatic
Methoxytoluene	11.78	122	121+122		Aromatic
Indene	12.64	116	115+116		Aromatic
Benzaldehyde	13.35	106	77+106		Aromatic
Dihydrobenzofuran	26.19	120	91+119+120		Aromatic
Limonene	7.22	136	93		Terpene
Phytol	20.00	276	95+123	Chlorophyll	Terpene
Unknown aliphatic	22.82		58+71		aliphatic
Aceton	2.46	58	43		
2-Propenal	2.60	56	55+56		
Methanol	2.88	32	29+31+32		
3-Buten-2-one	3.39	70	55+70		
2,3-Butandione	3.67	86	69+86		
3-Penten-2-one	3.89	86	69+86		
2-Butanal	4.56	70	69+70		
2,3-Pentadione	4.77	100	57+100		
Hexanal	5.16	82	56+72+82		
1-Penten-3-one	11.28	84	55+84		
Hexan-2,4-dion	23.92	114	56+84+114		
unknown	15.98		119+134		
Unknown	20.85		81		
Unknown	20.86		82+95		
Unknown	22.43		98+128		
Unknown	27.76		138		

Table 4. caption

	PC1	PC2	PC3
al	0.867	0.029	0.018
C	-0.414	-0.813	0.009
L	0.572	-0.693	-0.145
lip	0.034	0.181	-0.138
N	0.663	0.227	-0.293
non	0.644	0.025	-0.112
Ph	-0.197	0.922	0.113
phytol	-0.001	0.396	-0.266
unk	-0.808	0.388	0.157
al	0.779	0.286	0.290
al0	0.793	0.063	0.063
al1	0.917	-0.067	-0.105
ar	0.229	0.543	-0.674
bf	-0.793	0.412	0.144
cp	0.937	-0.166	0.066
f	-0.807	-0.494	-0.241
fa	0.034	0.181	-0.138
g	0.545	-0.737	-0.045
ind	0.628	0.564	-0.221
N-me-pyr	0.506	-0.049	-0.818
o	0.013	-0.203	0.408
p	0.719	0.358	-0.416
ph	-0.197	0.922	0.113
phytol	-0.001	0.396	-0.266
pyridol	0.272	-0.123	0.009
s	0.878	-0.137	0.408
short	0.695	-0.217	0.195
sy	0.552	-0.508	-0.332
ter	-0.882	0.186	-0.230
unk	-0.776	-0.522	0.089

```

    graphcorr2, fig=T, echo=F, results=hide, width=24, height=16)
pdf("corplot2.pdf", width=9, height=6) h3.pch<-c(rep(21,5), rep(22,5), rep(23,5), rep(24,5))
h3.col<-c(rep(colscale[1],5),rep(colscale[2],5),rep(colscale[3],5),rep(colscale[4],5))
var1<-alldataCNinbal[alldatadays==181] var2<-alldataCPinbal[alldatadays==181]
var3<-alldataNPinbal[alldatadays==181] var4<-hmv.procLCIvar5 <- hmv.procLCdec
var1lab<- expression("C:N"[litter:microbial]) var2lab<- expression("C:P"[litter:microbial]) var3lab<-
expression("N:P"[litter:microbial]) var4lab<- expression(paste(Delta, "LCI"[pyr])) var5lab<- "Lignin
decomposition /Carbohydrate decomposition"
par(cex=1, cex.axis=1, cex.lab=1, mar=c(0,0,0,0), tck=.01, las=1, mgp=c(3,0.3,0))
layout(matrix(c(1,2,3,4,5,6), 2,3, byrow=T))
m <- rbind( c(0.12, 0.385, 0.56, 0.98), c(0.39, 0.655, 0.56, 0.98), c(0.66, 0.925, 0.56, 0.98), c(0.12, 0.385,
0.135, 0.555), c(0.39, 0.655, 0.135, 0.555), c(0.66, 0.925, 0.135, 0.555), c(0.28, 0.38, 0.84, 0.975), c(0.55,
0.65, 0.84, 0.975), c(0.145, 0.245, 0.41, 0.545), c(0.415, 0.515, 0.41, 0.545) ) split.screen(m) screen(1)
par(mar=c(3,4,2,0.8), new=F, oma=c(0,0,0,0)) xlim=c(min(var1, na.rm=T)-(max(var1, na.rm=T)-
min(var1, na.rm=T))*0.2,max(var1, na.rm=T)+(max(var1, na.rm=T)- min(var1, na.rm=T))*0.2)
ylim=c(min(var4, na.rm=T)-(max(var4, na.rm=T)- min(var4, na.rm=T))*0.1,max(var4,
na.rm=T)+(max(var4, na.rm=T)- min(var4, na.rm=T))*0.2) corplot(var1, var4, xlab="", xaxt="n",
ylab="", bg=h3.col, pch=h3.pch, textpos="left", xlim=xlim, ylim=ylim)
?axis axis(4, label=F) axis(1, label=F) mtext(var4lab, side=2, las=0, cex=1.2, padj=-2)
screen(2)
par(mar=c(3,2.4,2,2.4)) xlim=c(min(var2, na.rm=T)-(max(var2, na.rm=T)- min(var2,
na.rm=T))*0.2,max(var2, na.rm=T)+(max(var2, na.rm=T)- min(var2, na.rm=T))*0.2) ylim=c(min(var4,
na.rm=T)-(max(var4, na.rm=T)- min(var4, na.rm=T))*0.1,max(var4, na.rm=T)+(max(var4, na.rm=T)-
min(var4, na.rm=T))*0.2) corplot(var2, var4, xlab="", ylab="", xaxt="n", yaxt="n", bg=h3.col,
pch=h3.pch, textpos="left", xlim=xlim, ylim=ylim) axis(1, label=F) axis(2, label=F) axis(4, label=F)
screen(3)
par(mar=c(3,0.8,2,4))
xlim=c(min(var3, na.rm=T)-(max(var3, na.rm=T)- min(var3, na.rm=T))*0.2,max(var3,
na.rm=T)+(max(var3, na.rm=T)- min(var3, na.rm=T))*0.2) ylim=c(min(var4, na.rm=T)-(max(var4,
na.rm=T)- min(var4, na.rm=T))*0.1,max(var4, na.rm=T)+(max(var4, na.rm=T)- min(var4,
na.rm=T))*0.2)
corplot(var3, var4, xlab="", ylab="", xaxt="n", yaxt="n", bg=h3.col, pch=h3.pch, xlim=xlim, ylim=ylim)
axis(1, label=F) axis(2, label=F) axis(4)
screen(4)
xlim=c(min(var1, na.rm=T)-(max(var1, na.rm=T)- min(var1, na.rm=T))*0.2,max(var1,
na.rm=T)+(max(var1, na.rm=T)- min(var1, na.rm=T))*0.2) ylim=c(min(var5, na.rm=T)-(max(var5,
na.rm=T)- min(var5, na.rm=T))*0.1,max(var5, na.rm=T)+(max(var5, na.rm=T)- min(var5,
na.rm=T))*0.2)
corplot(var1, var5, xlab=var1lab, ylab="", bg=h3.col, pch=h3.pch, xaxt="n",yaxt="n", xlim=xlim,
ylim=ylim) axis(4, label=F) axis(1) axis(2) axis(3, label=F)
mtext(var5lab, side=2, cex=1, las=0, padj=-1) mtext(var1lab, side=1, cex=1, padj=2)
?mtext
screen(5)
xlim=c(min(var2, na.rm=T)-(max(var2, na.rm=T)- min(var2, na.rm=T))*0.2,max(var2,
na.rm=T)+(max(var2, na.rm=T)- min(var2, na.rm=T))*0.2) ylim=c(min(var5, na.rm=T)-(max(var5,
na.rm=T)- min(var5, na.rm=T))*0.1,max(var5, na.rm=T)+(max(var5, na.rm=T)- min(var5,
na.rm=T))*0.2)
par(mar=c(5,2.4,0,2.4)) corplot(var2, var5, xlab="", ylab="", bg=h3.col, pch=h3.pch, xaxt="n",yaxt="n",
xlim=xlim, ylim=ylim) axis(1) axis(2, label=F) axis(3, label=F) axis(4, label=F) mtext(var2lab, side=1,
cex=1, padj=2)
screen(6) par(mar=c(5,0.8,0,4))
xlim=c(min(var3, na.rm=T)-(max(var3, na.rm=T)- min(var3, na.rm=T))*0.2,max(var3,
na.rm=T)+(max(var3, na.rm=T)- min(var3, na.rm=T))*0.2) ylim=c(min(var5, na.rm=T)-(max(var5,
na.rm=T)- min(var5, na.rm=T))*0.1,max(var5, na.rm=T)+(max(var5, na.rm=T)- min(var5,
na.rm=T))*0.2)
corplot(var3, var5, xlab=var3lab, ylab="", bg=h3.col, pch=h3.pch, xaxt="n",yaxt="n", xlim=xlim,

```

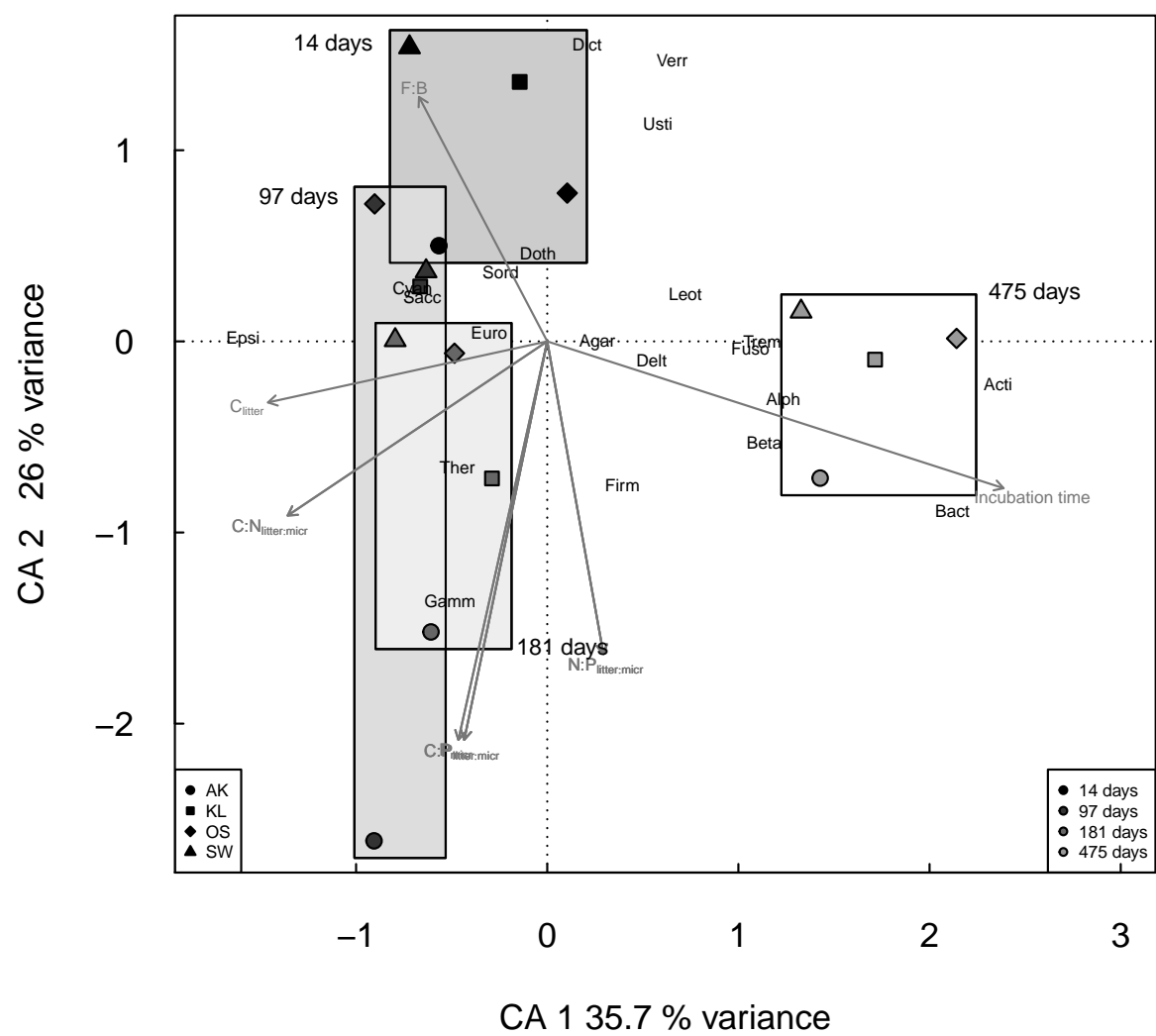


Table 5. Results of correlation analysis (R) between lignin and carbohydrate decomposition and other decomposition processes (mass loss, respiration), extracellular enzyme activities, litter chemistry, and litter and microbial biomass C:N:P stoichiometry. Significant ($p < 0.05$) correlations are presented in bold. Changes in litter chemistry (lignin and carbohydrate decomposition) were calculated between 0 and 181 days, other data were measured after 181 days. ΔLCI_{pyr} - difference in the pyr-GC/MS based lignocellulose index (lignin: (lignin + carbohydrates)), L_{degr} , Ch_{degr} - % of initial lignin or carbohydrate loss, L/C_{degr} , Ch/C_{degr} - % lignin or carbohydrates loss per % carbon respired, $L : Ch_{degr}$ - lignin loss : carbohydrate loss, PHENOX:CELL - Potetial phenoloxidase activity : potential cellulase activity.

	ΔLCI_{pyr}	$L_{\%loss}$	$Ch_{\%loss}$	$L : C_{\%loss}$	$Ch : C_{\%loss}$	$L : Ch_{\%loss}$	PHENOX:CELL
Massloss	0.245	-0.328	0.106	-0.201	0.125	-0.081	0.048
Actual respiration	0.565	-0.543	0.392	-0.503	0.453	-0.458	-0.294
Accumulated Respiration	0.114	0.400	0.446	0.208	0.258	0.098	-0.251
Cellulase activity	0.803	-0.431	0.801	-0.497	0.664	-0.589	-0.436
Protease activity	0.264	-0.132	0.274	-0.157	0.301	-0.270	-0.260
Phosphatase activity	0.663	-0.170	0.795	-0.312	0.677	-0.559	-0.490
Chitinase activity	0.776	-0.302	0.851	-0.407	0.702	-0.556	-0.418
Phenoloxidase activity	0.737	-0.415	0.719	-0.449	0.552	-0.484	-0.305
Peroxidase activity	0.677	-0.412	0.639	-0.438	0.470	-0.435	-0.173
N mineralization	0.650	-0.167	0.739	-0.299	0.527	-0.387	-0.282
Nitrification	0.732	-0.380	0.740	-0.432	0.621	-0.499	-0.369
P mineralization	0.684	-0.544	0.596	-0.576	0.414	-0.478	-0.212
C litter	-0.578	0.604	-0.368	0.643	-0.618	0.698	0.525
extractable C	0.790	-0.348	0.841	-0.440	0.678	-0.552	-0.411
N litter	0.503	-0.140	0.587	-0.187	0.366	-0.203	-0.119
extractable N	0.681	-0.148	0.836	-0.282	0.625	-0.474	-0.415
P litter	0.617	-0.732	0.358	-0.657	0.375	-0.466	-0.150
extractable P	0.565	-0.543	0.392	-0.503	0.453	-0.458	-0.294
C:N litter	-0.567	0.170	-0.654	0.230	-0.437	0.268	0.191
C:P litter	-0.493	0.734	-0.179	0.620	-0.270	0.384	0.088
N:P litter	-0.308	0.687	0.051	0.535	-0.125	0.269	0.013
C:N mic	0.799	-0.428	0.798	-0.514	0.678	-0.609	-0.583
C:P mic	0.833	-0.475	0.813	-0.561	0.725	-0.671	-0.564
N:P mic	0.740	-0.416	0.728	-0.508	0.715	-0.670	-0.545
C:N (litter:micr)	-0.771	0.285	-0.860	0.389	-0.709	0.529	0.562
C:P (litter:micr)	-0.839	0.775	-0.653	0.818	-0.707	0.849	0.587
N:P (litter:micr)	-0.638	0.800	-0.345	0.749	-0.491	0.651	0.343
Fungi/bacteria(qPCR)	0.079	-0.024	0.087	-0.066	0.135	-0.072	0.199
Fungi/bacteria (metaproteome)	0.998	-0.854	0.958	-0.882	0.801	-0.961	0.824

Table 6. Results of correlation analysis (R) between lignin and carbohydrate decomposition and other decomposition processes (mass loss, respiration), extracellular enzyme activities, litter chemistry, and litter and microbial biomass C:N:P stoichiometry. Significant ($p < 0.05$) correlations are presented in bold. Changes in litter chemistry (lignin and carbohydrate decomposition) were calculated between 181 and 475 days, other data were measured after 475 days. ΔLCI_{pyr} - difference in the pyr-GC/MS based lignocellulose index (lignin: lignin + carbohydrates), L_{degr} , Ch_{degr} - % of initial lignin or carbohydrate loss, L/C_{degr} , Ch/C_{degr} - % lignin or carbohydrates loss per % carbon respired, $L : Ch_{degr}$ - lignin loss : carbohydrate loss, PHENOX:CELL - Potetial phenoloxidase activity : potential cellulase activity.

	ΔLCI_{pyr}	$L_{\%loss}$	$Ch_{\%loss}$	$L : C_{\%loss}$	$Ch : C_{\%loss}$	$L : Ch_{\%loss}$	PHENOX:CELL
Massloss	0.068	0.582	0.708	0.005	0.279	-0.137	-0.444
Actual respiration	-0.273	0.826	0.773	0.238	0.216	0.043	-0.365
Accumulated Respiration	0.356	0.007	0.229	-0.274	0.119	-0.283	-0.334
Cellulase activity	-0.137	0.848	0.881	0.148	0.295	-0.081	-0.575
Protease activity	-0.086	0.448	0.455	0.160	0.316	-0.110	-0.456
Phosphatase activity	0.069	0.298	0.373	-0.102	-0.014	-0.115	-0.152
Chitinase activity	-0.086	0.643	0.671	0.167	0.253	-0.029	-0.580
Phenoloxidase activity	0.436	-0.248	-0.003	-0.221	0.505	-0.443	-0.483
Peroxidase activity	-0.385	0.173	-0.049	0.160	-0.510	0.382	0.546
N mineralization	0.078	0.009	0.062	-0.191	-0.113	-0.167	0.062
Nitrification	-0.320	0.630	0.567	0.090	-0.148	0.114	-0.105
P mineralization	-0.138	0.507	0.508	-0.136	-0.063	-0.128	0.043
C litter	0.177	-0.325	-0.264	-0.204	-0.289	0.024	0.501
extractable C	-0.086	0.829	0.890	0.073	0.218	-0.109	-0.538
N litter	-0.065	0.816	0.896	-0.004	0.172	-0.120	-0.431
extractable N	-0.084	0.799	0.859	0.076	0.224	-0.117	-0.533
P litter	-0.266	0.775	0.721	0.228	0.243	0.017	-0.359
extractable P	-0.273	0.826	0.773	0.238	0.216	0.043	-0.365
C:N litter	0.018	-0.798	-0.904	0.028	-0.204	0.155	0.488
C:P litter	0.317	-0.641	-0.536	-0.276	-0.216	-0.065	0.276
N:P litter	0.329	-0.330	-0.172	-0.294	-0.112	-0.146	0.042
C:N mic	0.093	-0.657	-0.703	-0.030	-0.315	0.251	0.569
C:P mic	0.312	-0.609	-0.505	-0.191	-0.071	-0.063	0.233
N:P mic	0.293	-0.378	-0.250	-0.185	0.048	-0.160	0.000
C:N(litter:micr)	-0.073	-0.363	-0.455	0.061	0.046	-0.051	0.027
C:P(litter:micr)	-0.077	-0.129	-0.192	-0.018	-0.241	0.100	0.150
N:P(litter:micr)	-0.091	0.058	0.009	0.007	-0.270	0.180	0.148
Fungi/bacteria(qPCR)	0.017	-0.236	-0.254	-0.089	-0.115	-0.003	0.161
Fungi : bacteria (metaproteome)	-0.369	0.986	0.972	0.254	0.484	-0.274	-0.601

Table 7. caption

dependent variable	predictor	t	df	p	cor
ΔLCI_{pyr}	$C : N_{litter:micr}$	-5.14	18	<0.001	-0.771
	residual	-2.89	17	0.010	-0.575
	residual	-2.92	17	0.098	-0.576
ΔLCI_{pyr}	$C : P_{litter:micr}$	-6.35	17	<0.001	-0.839
	residual	-1.72	17	0.104	-0.385
	residual	1.01	17	0.352	0.239
ΔLCI_{pyr}	$N : P_{litter:micr}$	-3.41	17	0.003	-0.638
	residual	-4.17	17	0.001	-0.711
	residual	-1.44	17	0.167	-0.331
% Lignin loss:%Ch loss	$C : N_{litter:micr}$	2.64	18	0.017	0.529
	residual	3.72	17	0.002	0.670
	residual	3.03	17	0.007	0.593
%Lignin loss:%Ch loss	$C : P_{litter:micr}$	6.62	17	<0.001	0.849
	residual	0.70	17	0.494	0.167
	residual	-1.01	17	0.326	-0.238
%Lignin loss:%Ch loss	$N : P_{litter:micr}$	3.54	17	<0.003	-0.651
	residual	2.81	17	0.012	0.564
	residual	1.46	17	0.164	0.333

Table 8. Correlations coefficients between correspondance analysis factors CA 1 and 2, litter and microbial stoichiometry and protein abundance of microbial taxa. Significant ($p < 0.05$) correlations are presented in bold.

	CA1	CA2
Incubation time	0.872	-0.281
Respiration	-0.158	0.601
NH4 conc.	0.037	0.029
NO3 conc.	0.584	-0.056
PO4 conc	0.090	0.321
C litter	-0.787	-0.172
N litter	-0.174	0.268
P litter	-0.162	0.367
C:N litter	-0.046	-0.265
C:P litter	0.070	-0.339
N:P litter	0.099	-0.230
C micr.	-0.078	0.016
N micr.	-0.251	-0.047
P micr.	-0.132	-0.590
C:N micr.	0.417	0.212
C:P micr.	0.077	0.589
N:P micr.	-0.296	0.446
C:N imbalance	-0.504	-0.338
C:P imbalance	-0.161	-0.773
N:P imbalance	0.109	-0.606
F:B prot.	-0.417	0.795
Dothideomycetes	-0.078	0.745
Eurotiomycetes	-0.578	0.083
Leotiomycetes	0.731	0.253
Saccharomycetes	-0.501	0.180
Sordariomycetes	-0.511	0.762
Agaricomycetes	0.167	-0.004
Tremellomycetes	0.723	-0.000
Ustilaginomycetes	0.188	0.370
Thermotogae	-0.336	-0.469
Bacteroidetes	0.638	-0.267
Actinobacteria	0.896	-0.085
Cyanobacteria	-0.319	0.122
Firmicutes	0.183	-0.350
Fusobacteria	0.227	-0.009
Verrucomicrobia	0.114	0.256
Dictyoglomi	0.027	0.200
Alphaproteobacteria	0.924	-0.232
Betaproteobacteria	0.766	-0.358
Gammaproteobacteria	-0.348	-0.929
Deltaproteobacteria	0.229	-0.043
Epsilonproteobacteria	-0.205	0.002

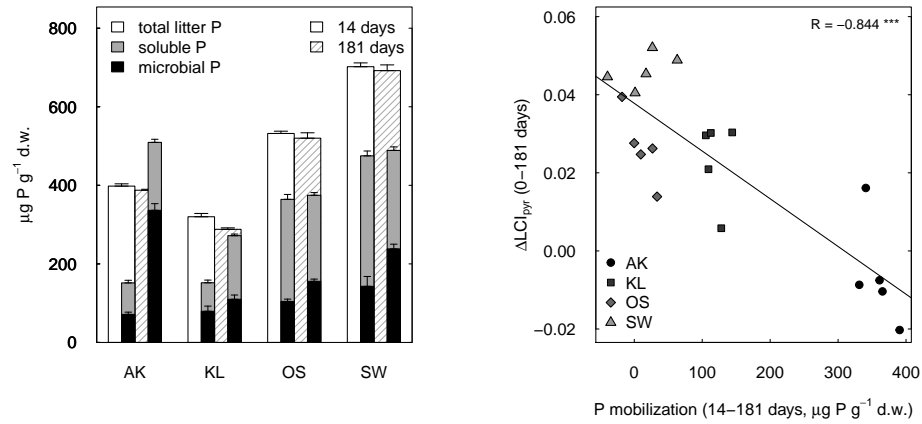


Figure 1. Mobilization of litter P Left: In lignin degrading litter (AK and KL) a net mobilization of Insoluble litter P into the fast turn-over P pools (soluble P and microbial biomass P) occurred over the first 6 months incubation. In non lignin-degrading litter (OS and SW) increases biomass P corresponded with decreases in soluble P, i.e., no additional insoluble P mobilized. Right: correlation between P mobilization and lignin accumulation, 0-6 months incubation. Beech litter was collected in: Schottenwald (SW), triangles; Ossiach (OS), diamonds; Klausenleopoldsdorf (KL), squares; Achenkirch (AK), circles. Error bars indicate standard errors (n=5).

